



IRSTI 29.19.03  
scientific article

DOI: <https://doi.org/10.32523/2616-6836-2024-148-3-117-125>

## Reanalysis of $^{20}\text{Ne} + ^{24}\text{Mg}$ elastic scattering angular distributions within various interaction potentials

Sh. Hamada<sup>1</sup> 

<sup>1</sup>Faculty of Science, Tanta University, Tanta, Egypt

(E-mail: [sh.m.hamada@science.tanta.edu.eg](mailto:sh.m.hamada@science.tanta.edu.eg))

**Abstract:** The angular distributions (ADs) for  $^{20}\text{Ne}$  elastically scattered from a  $^{24}\text{Mg}$  target were measured experimentally many years ago at  $E_{lab} = 50\text{--}100$  MeV. Unfortunately, these data received little attention and were analyzed only from a phenomenological perspective at that time. This work is essentially devoted to investigating these data from a microscopic point of view, with a special interest given to the probable  $\alpha + ^{16}\text{O}$  cluster structure of the  $^{20}\text{Ne}$  nucleus. The considered data are fairly well reproduced by the implemented potentials. The study demonstrated the success of the proposed  $\alpha + ^{16}\text{O}$  cluster model of the  $^{20}\text{Ne}$  nucleus in reproducing the considered  $^{20}\text{Ne} + ^{24}\text{Mg}$  ADs over a wide range of energies.

**Keywords:** Density distributions, Elastic scattering, Optical potential, Cluster folding, Brazilian Nuclear potential.

Received 29.08.2024. Revised 04.09.2024. Accepted 05.09.2024. Available online 30.09.2024

### Introduction

The traditional view of the nucleus is that it has a uniform distribution of neutrons and protons. However, from the early days of nuclear research, it has been recognized that nucleon clusters, or nuclear clustering, might be crucial for a deeper understanding of nuclear interactions and structure. In the 1950s, Morinaga [1] made a bold prediction that alpha particles could align linearly. He suggested that cluster structures would not be present in the ground state of a nucleus but would emerge as the internal energy of the nucleus increased. Thus, a nucleus needs a certain amount of energy to develop a cluster structure, with these structures becoming evident near or just below the cluster decay threshold energy. Ikeda et al. [2] expected that the cluster structure would become most pronounced at excitation energy ( $Ex$ ) corresponding to specific decay thresholds.

Experimental evidence supporting the concept of clusterization in light nuclei is detailed in M. Freer's work [3]. A clear example is the two alpha-particle system in  $^8\text{Be}$ , where the strong

alpha-particle binding energy ( $\sim 28$  MeV) implies that  ${}^6\text{Li}$  and  ${}^7\text{Li}$  nuclei are likely to form  $\alpha + \text{d}$  and  $\alpha + \text{t}$  cluster structures, respectively. The Hoyle state in  ${}^{12}\text{C}$ , observed at  $E_x = 7.65$  MeV, is an exemplary cluster state. Hoyle [4] had predicted this state to explain the cosmic abundance of carbon, and Cook [5] detected it at an energy very close to Hoyle's prediction.

The  ${}^{20}\text{Ne} + {}^{24}\text{Mg}$  system is particularly intriguing and could provide valuable insights for extracting spectroscopic factors for the  ${}^{20}\text{Ne} \rightarrow {}^{16}\text{O} + \alpha$  and  ${}^{24}\text{Mg} \rightarrow {}^{20}\text{Ne} + \alpha$  configurations. However, only a few studies [6, 7] have investigated this system, and these studies used predominantly phenomenological approaches. In Ref. [6], angular distributions (ADs) for the  ${}^{24}\text{Mg} ({}^{20}\text{Ne}, {}^{20}\text{Ne}) {}^{24}\text{Mg}$  at  $E_{lab} = 50\text{-}100$  MeV were measured in the angular range  $10^\circ < \theta_{c.m.} < 75^\circ$ . These data were described using optical model potentials (OMPs). Reduced absorption and  $\alpha$ -cluster transfer were discussed theoretically but not observed experimentally at this energy range. Volume integrals and total reaction cross-sections for the potentials were also determined. Ref. [7] involved measurements of ADs for a  ${}^{20}\text{Ne}$  ion beam at 40 MeV elastically scattered from a  ${}^{24}\text{Mg}$  target. The measured ADs exhibited oscillations associated with the  ${}^{24}\text{Mg} ({}^{20}\text{Ne}, {}^{24}\text{Mg}) {}^{20}\text{Ne}$  reaction. An  $\alpha$ -spectroscopic factor (SF) of  $0.08 \pm 0.02$  was derived from the analysis, considering the coherent sum of scattering amplitudes from elastic scattering and  $\alpha$ -transfer.

In a previous study [8], the  ${}^{20}\text{Ne} + {}^{24}\text{Mg}$  ADs were analyzed using the São Paulo potential (SPP2) and a cluster folding potential (CFP). The latter was generated based on available phenomenological OMPs for the  $\alpha + {}^{24}\text{Mg}$  and  ${}^{16}\text{O} + {}^{24}\text{Mg}$  channels. In the current study, the  ${}^{20}\text{Ne} + {}^{24}\text{Mg}$  ADs are reanalyzed using a microscopic CFP and the Brazilian Nuclear Potential (BNP), which is independent of both projectile energy and relative velocity. The CFP used in this study was generated from microscopic  $\alpha + {}^{24}\text{Mg}$  and  ${}^{16}\text{O} + {}^{24}\text{Mg}$  potentials, rather than the phenomenological ones used in Ref. [8].

Overall, the concept of clusterization offers a valuable framework for understanding complex nuclear systems and enhances our knowledge of nuclear physics. This work focuses on exploring the probable  $\alpha + {}^{16}\text{O}$  structure model of  ${}^{20}\text{Ne}$  nucleus and its ability to reproduce the  ${}^{20}\text{Ne} + {}^{24}\text{Mg}$  ADs across a broad energy range within this model. The manuscript is organized as follows: Section II presents the potentials used, Section III covers the analyses and discussion of the results, and Section IV provides a summary and conclusions.

## Implemented theoretical methods

The available experimental ADs data for  ${}^{20}\text{Ne} + {}^{24}\text{Mg}$  system at  $E_{lab} = 50, 60, 80, 90,$  and  $100$  MeV [6] are initially reanalyzed using the BNP, which incorporates the density distributions of the interacting nuclei. Then, the full microscopic cluster folding potential (CFP) is employed to evaluate the accuracy of reproducing the  ${}^{20}\text{Ne} + {}^{24}\text{Mg}$  data using the  $\alpha + {}^{16}\text{O}$  model for  ${}^{20}\text{Ne}$ , a model that has previously demonstrated significant success in describing various nuclear systems induced by  ${}^{20}\text{Ne}$  [8-10].

## BNP

To eliminate parameter ambiguities associated with OMP calculations, the more microscopic Brazilian Nuclear potential (BNP) was employed to generate the real part of the potential. This was done by folding the projectile ( $\rho_p$ ) and target ( $\rho_t$ ) density distributions, obtained from the Dirac-Hartree-Bogoliubov model [11], with an effective potential. Recently, L.C. Chamon et al. [12] suggested two models for the nuclear potential between interacting nuclei: the São Paulo potential (SPP2), which depends on the relative velocity of the nuclei, and the BNP, which is independent of both projectile energy and relative velocity. The effective nucleon-nucleon ( $NN$ ) interactions for the SPP2 and BNP are given by the following formulas:

$$v_{NN}^{SPP2}(R) = -U_o e^{\left(\frac{-R}{a}\right)^2} e^{\left(\frac{-4v^2}{c^2}\right)} \quad (1)$$

with  $U_o = 735.813$  MeV,  $a = 0.5$  fm,  $v$  representing the relative velocity between the interacting nuclei, and  $c$  being the speed of light.

$$v_{NN}^{BNP}(R) = -U_o e^{\left(\frac{-R}{a}\right)^2} \quad (2)$$

with  $U_o = 87.226$  MeV and  $a = 0.95$  fm.

Data optimization was performed by minimizing the  $\chi^2$  value, which quantifies the discrepancy between the data and the theoretical results. The calculations and parameter optimization were carried out using the **FRESCO** and **SFRESCO** code [13]. It is worth noting that in a previous study [8], these ADs data for the  $^{20}\text{Ne} + ^{24}\text{Mg}$  system were analyzed within the SPP2 potential. Therefore, it is of interest to compare the SPP2 and BNP potentials in reproducing the considered data.

## CFP

The study advances by aiming to match the experimental data for the elastic scattering of  $^{20}\text{Ne} + ^{24}\text{Mg}$  ADs using a cluster folding model (CFM). This approach is inspired by the  $\alpha + ^{16}\text{O}$  cluster structure in the ground state of the  $^{20}\text{Ne}$ . In the CFM framework, both the real and imaginary components of the potential are developed using the cluster folding technique. To conduct the calculations for the  $^{20}\text{Ne} + ^{24}\text{Mg}$  system, it is essential to establish the potentials for the  $\alpha + ^{24}\text{Mg}$  and  $^{16}\text{O} + ^{24}\text{Mg}$  channels as well as the binding potential for the  $\alpha + ^{16}\text{O}$  configuration in the  $^{20}\text{Ne}$  nucleus. The real and imaginary components of the  $^{20}\text{Ne} + ^{24}\text{Mg}$  potential are derived from these  $\alpha + ^{24}\text{Mg}$  and  $^{16}\text{O} + ^{24}\text{Mg}$  potentials as follows:

$$V^{CF}(\mathbf{R}) = \int \left[ V_{\alpha + ^{24}\text{Mg}}\left(\mathbf{R} - \frac{4}{5}\mathbf{r}\right) + V_{^{16}\text{O} + ^{24}\text{Mg}}\left(\mathbf{R} + \frac{1}{5}\mathbf{r}\right) \right] |\chi_0(\mathbf{r})|^2 d\mathbf{r}, \quad (3)$$

$$W^{CF}(\mathbf{R}) = \int \left[ W_{\alpha+^{24}\text{Mg}}\left(\mathbf{R} - \frac{4}{5}\mathbf{r}\right) + W_{^{16}\text{O}+^{24}\text{Mg}}\left(\mathbf{R} + \frac{1}{5}\mathbf{r}\right) \right] |\chi_0(\mathbf{r})|^2 d\mathbf{r}, \quad (4)$$

where  $V_{\alpha+^{24}\text{Mg}}$ ,  $V_{^{16}\text{O}+^{24}\text{Mg}}$ ,  $W_{\alpha+^{24}\text{Mg}}$ , and  $W_{^{16}\text{O}+^{24}\text{Mg}}$  are the potentials for  $\alpha+^{24}\text{Mg}$  and  $^{16}\text{O}+^{24}\text{Mg}$  channels, which reproduce the experimental data at  $E_{\alpha} \approx 1/5 E_{Ne}$  and  $E^{16\text{O}} \approx 4/5 E_N$  prepared within the BNP using standard normalizations of 1.0 and 0.78 for the real and imaginary potential parts, respectively. The term is the intercluster wave function for the relative motion of  $\alpha$  and  $^{16}\text{O}$  in the ground state of  $^{20}\text{Ne}$ , and  $\mathbf{r}$  is the relative coordinate between the centers of mass of  $\alpha$  and  $^{16}\text{O}$ . The bound state form factor  $\alpha + ^{16}\text{O}$  represents a  $5S$  state, is taken from Ref. [14]. The real and imaginary components of the cluster folding potential used in the current work are illustrated in Fig. 1.

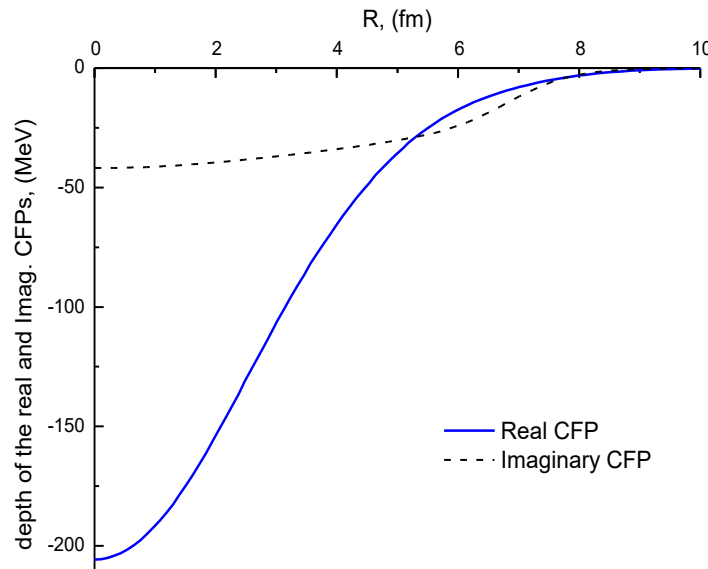


Fig. 1: The real and imaginary CFPs for the  $^{20}\text{Ne} + ^{24}\text{Mg}$  system

## Results and Discussions

### $^{20}\text{Ne} + ^{24}\text{Mg}$ data analysis using BNP

As depicted in Fig. 2, the experimental ADs for  $^{20}\text{Ne} + ^{24}\text{Mg}$  are compared with theoretical calculations using a real BNP component and an imaginary potential, which is a factor multiplied by the real BNP. This approach, referred to as BNP Real + BNP Imag, involves fitting the data with two adjustable parameters:  $N_R$  and  $N_I$ , which are normalization factors for the real and imaginary BNP strengths. The optimal extracted parameters using this method are listed in Table I. The total potential is expressed as follows:

$$U(R) = V_C(R) - N_R V^{BNP}(R) - i N_I V^{BNP}(R) \quad (5)$$

The agreement between the data and theoretical calculations is generally good across the entire angular range, as shown in Fig. 2, using the potential parameters listed in Table I. The data is well fitted using an average extracted  $N_R$  and  $N_I$  values are  $0.74 \pm 0.14$  and  $0.75 \pm 0.1$ , respectively, which are close to the previously extracted values  $0.87 \pm 0.18$  and  $0.75 \pm 0.1$  from previous analysis [8] within SPP2. The experimental angular distribution reveals a Coulomb-nuclear interference peak, which shifts toward smaller scattering angles as the bombarding energy increases.

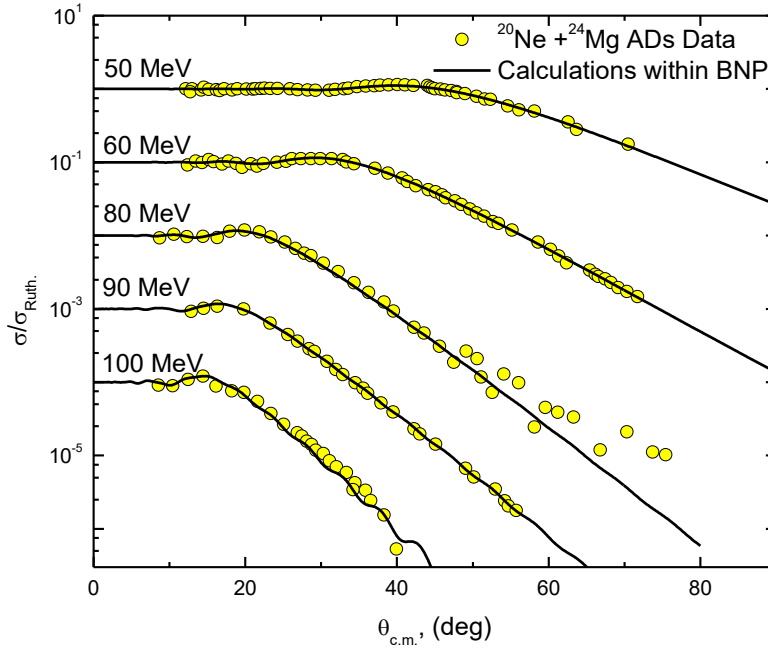


Fig. 2: Comparison between  $^{20}\text{Ne} + ^{24}\text{Mg}$  ADs and calculations within BNP at  $E_{lab} = 50\text{-}100$  MeV

### $^{20}\text{Ne} + ^{24}\text{Mg}$ data analysis using CFM

As illustrated in Fig. 3, the comparison between the experimental ADs for the  $^{20}\text{Ne} + ^{24}\text{Mg}$  system and the theoretical calculations using CFP model is quite accurate when employing the optimal extracted parameters listed in Table I. In this analysis, the data is fitted using two parameters  $N_R$  and  $N_I$ , which represent the normalization factors for the real and imaginary parts of the CFP, as shown in Fig. 1. The total potential is described by the following form:

$$U(R) = V_C(R) - N_R V^{CFP}(R) - i N_I V^{CFP}(R) \quad (6)$$

The average values extracted for  $N_R$  and  $N_I$  within the CFP model are  $0.81 \pm 0.09$  and  $0.86 \pm 0.38$ , respectively. While those extracted from previous study [8] are  $0.61 \pm 0.08$  and  $1.46 \pm 0.26$ .

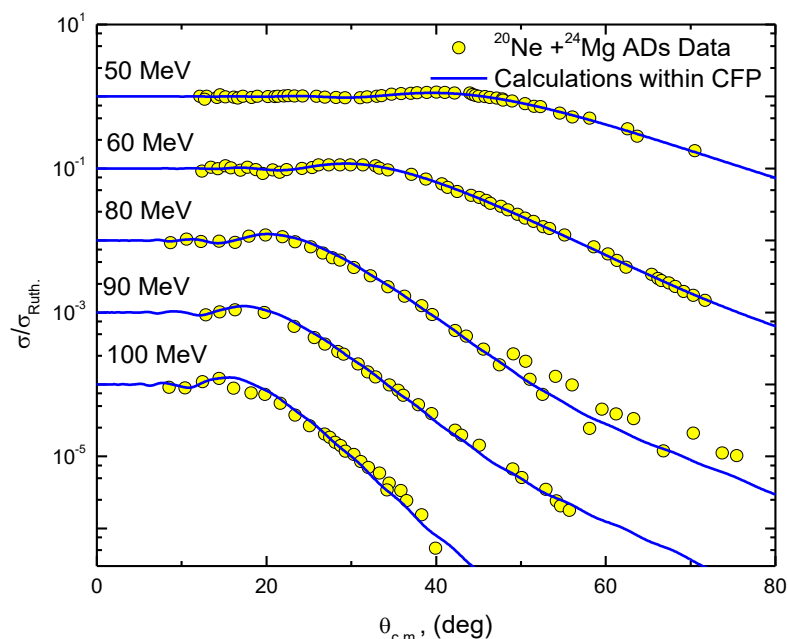


Fig. 3: Comparison between  $^{20}\text{Ne}+^{24}\text{Mg}$  ADs and calculations within CFP at  $E_{\text{lab}} = 50\text{-}100$  MeV

Table I: Optimal potential parameters for  $^{20}\text{Ne} + ^{24}\text{Mg}$  system at different energies extracted from the analyses within BNP and CFP

$E_{\text{lab}}$ (MeV)	Model	$N_R$	$N_I$	$\chi^2/N$
50	BNP	0.57	0.60	0.11
	CFP	0.79	1.26	0.08
60	BNP	0.69	0.74	0.19
	CFP	0.97	1.28	0.20
80	BNP	0.81	0.86	5.95
	CFP	0.79	0.64	4.85
90	BNP	0.67	0.83	0.18
	CFP	0.77	0.66	1.42
100	BNP	0.94	0.703	4.31
	CFP	0.75	0.45	4.30

## Summary

In summary, the angular distributions for elastic scattering of stable  $^{20}\text{Ne}$  a  $^{24}\text{Mg}$  target at energies ranging from 50 to 100 MeV show a classical Fresnel diffraction scattering pattern, as depicted in Figs. 2 and 3. However, a distinct deviation from this pattern is observed in

the case of elastic scattering involving weakly-bound nuclei, such as  $^{11}\text{Be}$  one-neutron halo nucleus [15], when interacting with different targets like  $^{64}\text{Zn}$  [16],  $^{120}\text{Sn}$  [17],  $^{197}\text{Au}$  [18], and  $^{209}\text{Bi}$  [19]. These interactions exhibit significant suppression of the Fresnel peak due to the break-up effects. Theoretical calculations within CFM, which is based on the  $\alpha + ^{16}\text{O}$  cluster structure for  $^{20}\text{Ne}$ , successfully reproduce the considered data, providing evidence supporting this proposed structural model for the  $^{20}\text{Ne}$  nucleus.

## References

1. H. Morinaga. Interpretation of Some of the Excited States of  $4n$  Self-Conjugate Nuclei // *Phys. Rev.* 101, 254 (1956), DOI: <https://doi.org/10.1103/PhysRev.101.254>.
2. K. Ikeda, N. Tagikawa, and H. Horiuchi. The Systematic Structure-Change into the Molecule-like Structures in the Self-Conjugate  $4n$  Nuclei // *Prog. Theo. Phys. Suppl.* E68, 464-475 (1968), DOI: <https://doi.org/10.1143/PTPS.E68.464>.
3. M. Freer. The clustered nucleus-cluster structures in stable and unstable nuclei // *Reports on Progress in Physics* 70, 2149 (2007), DOI: [10.1088/0034-4885/70/12/R03](https://doi.org/10.1088/0034-4885/70/12/R03)
4. F. Hoyle. On Nuclear Reactions Occuring in Very Hot STARS. I. the Synthesis of Elements from Carbon to Nickel // *Astrophys. J. Suppl.* 1, 121-146 (1954), DOI: [10.1086/190005](https://doi.org/10.1086/190005)
5. C. Cook, W. A. Fowler and T. Lauritsen. 12B, 12C, and the Red Giants // *Phys. Rev.* 107, 508 (1957), DOI: <https://doi.org/10.1103/PhysRev.107.508>
6. P. Belery, Th. Delbar, Gh. Grégoire, K. Grotowski, N. S. Wall, T. Kozik, and S. Micek. Elastic scattering of  $^{20}\text{Ne} + ^{24}\text{Mg}$  at  $E_{\text{lab}} = 50, 60, 80, 90,$  and  $100$  MeV // *Phys. Rev. C* 23, 2503 (1981), DOI: <https://doi.org/10.1103/PhysRevC.23.2503>
7. W. J. Naudé, H. S. Bradlow, O. Dietzsch, A. A. Pilt, W. D. M. Rae and D. Sinclair. Elastic scattering of  $^{20}\text{Ne}$  on  $^{24}\text{Mg}$  // *Z. Phys. A - Atoms and Nuclei* 311, 297-302 (1983), DOI: <https://doi.org/10.1007/BF01415684>
8. Sh. Hamada, A.H. Al-Ghamdi, Arafa A. Alholaisi, Awad A. Ibraheem, N. Amangeldi, Y. Abdou. Analysis of elastic scattering of  $^6, ^7\text{Li}$  and  $^{20}\text{Ne}$  from  $^{24}\text{Mg}$  nucleus using microscopic potentials // *Int. J. Mod. Phys. E* 32, 2350015 (2023), DOI: [10.1142/S0218301323500155](https://doi.org/10.1142/S0218301323500155)
9. Sh. Hamada, N. Keeley, K. W. Kemper and K. Rusek. Cluster folding analysis of  $^{20}\text{Ne} + ^{16}\text{O}$  elastic transfer // *Phys. Rev. C* 97, 054609 (2018), DOI: [10.1103/PhysRevC.97.054609](https://doi.org/10.1103/PhysRevC.97.054609)
10. Sh. Hamada, Nourhan M. Elmedalaa, I. Bondouk, N. Darwish, Awad A. Ibraheem. Role of  $\alpha$ -Cluster Transfer in the Formation of  $^{20}\text{Ne} + ^{16}\text{O}$  Cross-Sections at Backward Angles // *Braz. J. Phys.* 51, 780-787 (2021) 3, DOI: [10.1007/s13538-021-00900-z](https://doi.org/10.1007/s13538-021-00900-z)
11. B. V. Carlson and D. Hirata. Dirac-Hartree-Bogoliubov approximation for finite nuclei // *Phys. Rev. C* 62, 054310 (2000), DOI: <https://doi.org/10.1103/PhysRevC.62.054310>
12. L. C. Chamon, B. V Carlson, and L. R. Gasques. São Paulo potential version 2 (SPP2) and Brazilian nuclear potential (BNP) // *Comput. Phys. Commun.* 267, 108061 (2021), DOI: <https://doi.org/10.1016/j.cpc.2021.108061>
13. I. J. Thompson. Coupled reaction channels calculations in nuclear physics // *Comput. Phys. Rep.* 7, 167 (1988), DOI: [https://doi.org/10.1016/0167-7977\(88\)90005-6](https://doi.org/10.1016/0167-7977(88)90005-6)
14. B. Buck, J. C. Johnston, A. C. Merchant, S. M. Perez. Unified treatment of scattering and cluster structure in  $\alpha$ -closed shell nuclei:  $^{20}\text{Ne}$  and  $^{44}\text{Ti}$  // *Phys. Rev. C* 52, 1840 (1995), DOI: <https://doi.org/10.1103/PhysRevC.52.1840>

15. T. Aumann, A. Navin, D. P. Balamuth, D. Bazin, B. Blank, B. A. Brown, J. E. Bush, J. A. Caggiano, B. Davids, T. Glasmacher, V. Guimarães, P. G. Hansen, R. W. Ibbotson, D. Karnes, J. J. Kolata, V. Maddalena, B. Pritychenko, H. Scheit, B. M. Sherrill, J. A. Tostevin. One-Neutron Knockout from Individual Single-Particle States of  $^{11}\text{Be}$  // *Phys. Rev. Lett.* 84, 35 (2000), DOI: <https://doi.org/10.1103/PhysRevLett.84.35>
16. Di Pietro, V. Scuderi, A. M. Moro, L. Acosta, F. Amorini, M. J. G. Borge, P. Figuera, M. Fisichella, L. M. Fraile, J. Gomez-Camacho, H. Jeppesen, M. Lattuada, I. Martel, M. Milin, A. Musumarra, M. Papa, M. G. Pellegriti, F. Perez-Bernal, R. Raabe, G. Randisi, F. Rizzo, G. Scalia, O. Tengblad, D. Torresi, A. Maira Vidal, D. Voulot, F. Wenander, M. Zadro. Experimental study of the collision  $^{11}\text{Be} + ^{64}\text{Zn}$  around the Coulomb barrier // *Phys. Rev. C.* 85, 054607 (2012), DOI: <https://doi.org/10.1103/PhysRevC.85.054607>
17. L. Acosta, M. A. G. Alvarez, M. V. Andres, M. J. G. Borge, M. Cortes, J. M. Espino, D. Galaviz, J. Gomez-Camacho, A. Maira, I. Martel, A. M. Moro, I. Mukha, F. Perez-Bernal, E. Reillo, D. Rodriguez, K. Rusek, A. M. Sanchez-Benitez, O. Tengblad. Signature of a strong coupling with the continuum in  $^{11}\text{Be} + ^{120}\text{Sn}$  scattering at the Coulomb barrier // *Eur. Phys. J. A* 42, 461–464 (2009), DOI: [10.1140/epja/i2009-10822-6](https://doi.org/10.1140/epja/i2009-10822-6)
18. V. Pseudo, M. J. G. Borge, A. M. Moro, J. A. Lay, E. Nácher, J. Gómez-Camacho, O. Tengblad, L. Acosta, M. Alcorta, M. A. G. Alvarez, C. Andreoiu, P. C. Bender, R. Braid, M. Cubero, A. Di Pietro, J. P. Fernández-García, P. Figuera, M. Fisichella, B. R. Fulton, A. B. Garnsworthy, G. Hackman, U. Hager, O. S. Kirsebom, K. Kuhn, M. Lattuada, G. Marquínez-Durán, I. Martel, D. Miller, M. Moukaddam, P. D. O'Malley, A. Perea, M. M. Rajabali, A. M. Sánchez-Benítez, F. Sarazin, V. Scuderi, C. E. Svensson, C. Unsworth, and Z. M. Wang. Scattering of the Halo Nucleus  $^{11}\text{Be}$  on  $^{197}\text{Au}$  at Energies around the Coulomb Barrier // *Phys. Rev. Lett.* 118, 152502 (2017), DOI: <https://doi.org/10.1103/PhysRevLett.118.152502>
19. M. Mazzocco, C. Signorini, M. Romoli, R. Bonetti, A. De Francesco, A. De Rosa, M. DiPietro, L. Fortunato, T. Glodariu, A. Guglielmetti, G. Inglima, T. Ishikawa, H. Ishiyama, R. Kanungo, N. Khai, S. Jeong, M. La Commara, B. Martin, H. Miyatake, T. Motobayashi, T. Nomura, D. Pierroutsakou, M. Sandoli, F. Soramel, L. Stroe, I. Sugai, M. H. Tanaka, E. Vardaci, Y. Watanabe, A. Yoshida, K. Yoshida. Elastic scattering for the system  $^{11}\text{Be} + ^{209}\text{Bi}$  at Coulomb barrier energies // *Eur. Phys. J. Special Topics* 150, 37–40 (2007), DOI: [10.1140/epjst/e2007-00260-2](https://doi.org/10.1140/epjst/e2007-00260-2)

### Ш. Хамада

Факультет естественных наук, Университет Танта, Танта, Египет  
(E-mail: [sh.m.hamada@science.tanta.edu.eg](mailto:sh.m.hamada@science.tanta.edu.eg))

### Повторный анализ угловых распределений упругого рассеяния $^{20}\text{Ne} + ^{24}\text{Mg}$ в различных потенциалах взаимодействия

**Аннотация.** Угловые распределения (УР) для упруго рассеянного  $^{20}\text{Ne}$  от мишени  $^{24}\text{Mg}$  были измерены экспериментально много лет назад при  $E_{lab} = 50\text{--}100$  МэВ. К сожалению, эти данные получили мало внимания и были проанализированы только с феноменологической точки зрения в то время. Эта работа в основном посвящена исследованию этих данных с микроскопической точки зрения, при этом особый интерес уделяется вероятной кластерной структуре  $\alpha + ^{16}\text{O}$  ядра  $^{20}\text{Ne}$ . Рассмотренные данные достаточно хорошо воспроизводятся



реализованными потенциалами. Исследование продемонстрировало успешность предложенной кластерной модели  $\alpha + ^{16}\text{O}$  ядра  $^{20}\text{Ne}$  в воспроизведении рассматриваемых  $\text{AD}^{20}\text{Ne} + ^{24}\text{Mg}$  в широком диапазоне энергий.

**Ключевые слова:** распределение плотности, упругое рассеяние, оптический потенциал, кластерное соединение, Бразильский ядерный потенциал.

Номер(а) PACS: «21.10.Jx, 21.60.Cs, 24.10.Eq, 25.70.Ni»

### Ш. Хамада

Жаратылыстану факультеті, Танта университеті, Танта, Егунет  
(E-mail: sh.m.hamada@science.tanta.edu.eg)

### Әртүрлі өзара әрекеттесу потенциалдарында $^{20}\text{Ne} + ^{24}\text{Mg}$ серпімді шашыраудың бұрыштық үлестірімдерін қайта талдау

**Андатпа.**  $^{24}\text{Mg}$  нысанасынан серпімді шашыраңқы  $^{20}\text{Ne}$  үшін бұрыштық үлестірулер ( $\mu$ ) көптеген жылдар бұрын  $E_{lab} = 50-100$  МэВ кезінде эксперименталды түрде өлшенді. Өкінішке орай, бұл мәліметтерге назар аударылды және сол кезде тек феноменологиялық тұрғыдан талданды. Бұл жұмыс негізінен осы деректерді микроскопиялық тұрғыдан зерттеуге бағытталған,  $^{20}\text{Ne}$  ядросының  $\alpha + ^{16}\text{O}$  кластерлік құрылымына ерекше қызығушылық танытады. Қарастырылған деректер іске асырылған әлеуеттермен жақсы ойнатылады. Зерттеу ұсынылған  $\alpha + ^{16}\text{O}$   $^{20}\text{Ne}$  ядросының кластерлік моделінің қарастырылып отырған  $\text{ad}^{20}\text{Ne} + ^{24}\text{Mg}$ -ді кең энергия диапазонында ойнаудағы сәттілігін көрсетті.

**Түйін сөздер:** тығыздықтың таралуы, серпімді шашырау, оптикалық потенциал, кластерлік байланыс, бразилиялық ядролық потенциал

#### Information about authors:

**Sh. Hamada** – corresponding author, Faculty of Science, Tanta University, Tanta, Egypt

#### Сведения об авторах:

**Ш. Хамада** – автор для корреспонденции, Факультет естественных наук, Университет Танта, Танта, Египет.

#### Авторлар туралы мәліметтер:

**Ш. Хамада** – корреспондент автор, Жаратылыстану ғылымдары факультеті, Танта университеті, Танта, Египет



Copyright: © 2024 by the authors. Submitted for possible open access publication under the terms and conditions of the Creative Commons Attribution (CC BY NC) license (<https://creativecommons.org/licenses/by-nc/4.0/>).